IEEE Access
Multidisciplinary | Rapid Review | Open Access Journal

Received October 23, 2020, accepted November 10, 2020, date of publication November 16, 2020,
date of current version November 25, 2020.

Digital Object Identifier 10.1109/ACCESS.2020.3037966

Design and Testing of an Active Light Source Apparatus for Crop Growth Monitoring and Diagnosis

LILI YAO[1,2,3,4], RUSONG WU[5], SHUN WU[1,2], XIAOPING JIANG[1,2,3,4], YAN ZHU[1,2,3,4], WEIXING CAO[1,2,3,4], AND JUN NI[1,2,3,4]

[1]College of Agriculture, Nanjing Agricultural University, Nanjing 210095, China
[2]National Information Agricultural Engineering Technology Center, Nanjing Agricultural University, Nanjing 210095, China
[3]Engineering Research Center of Smart Agriculture, Ministry of Education, Nanjing Agricultural University, Nanjing 210095, China
[4]Jiangsu Collaborative Innovation Center for the Technology and Application of Internet of Things, Nanjing Agricultural University, Nanjing 210095, China
[5]Meyer Optoelectronic Technology Inc., Heifei 230000, China

Corresponding author: Jun Ni (nijun@njau.edu.cn)

This work was supported in part by the National Key Research and Development Program of China under Grant 2016YFD070030403, in part by the National Natural Science Foundation of China under Grant 31871524, in part by the Six Talent Peaks Project in Jiangsu Province under Grant XYDXX-049, and in part by the Priority Academic Program Development of Jiangsu Higher Education Institutions (PAPD) and the 111 Project (B16026).

ABSTRACT Portable spectrometers can extract crop growth information in a non-destructive, rapid, and efficient way. However, most existing instruments can only be used to collect spectral reflectance and calculate vegetation indices. They are costly and lack crop spectral monitoring models and diagnosis models; therefore, crop growth information cannot be directly output from these instruments. In this paper, an active light source apparatus for crop growth monitoring and diagnosis (CGMD) was developed based on the canopy shape characteristics and spectral monitoring mechanisms of row-cultivated crops. A modulated light source was used in this apparatus to effectively eliminate the interference of ambient light. At the same time, a high-pass filter was used in the apparatus to extract the canopy reflectance spectral information, which improves the signa-noise ratio. Crop canopy vegetation indexes—the normalized difference vegetation index (NDVI) and the ratio vegetation index (RVI)—and crop growth parameters—leaf area index (LAI), leaf dry weight (LDW), leaf nitrogen accumulation (LNA), and leaf nitrogen content (LNC)—were obtained in real time. The ambient light influence test and the comparison test of different test heights of the CGMD apparatus show that it has high test stability and can effectively overcome ambient light interference within the standard test height range. The rice and wheat experimental results demonstrated that the test results of the CGMD apparatus and the commercial Analytical Spectral Devices field spectrometer (Malvern Panalytical, Malvern, Worcs, UK) were consistent. Comparing the vegetation indexes and agronomic parameters obtained from the chemical analysis, the CGMD apparatus has a good predictive ability for LAI, LDW, LNC, and LNA.

INDEX TERMS Active light source, spectral monitoring, crop growth information, crop growth diagnosis.

I. INTRODUCTION

Implementing accurate crop production management is comprised of the acquisition of crop growth information, analysis and processing of this information, and the generation of fertilization prescriptions. Clearly, the accuracy of a crop management system relies on the access to crop growth information. The acquisition of traditional crop growth information mainly depended on visual observation and destructive field sampling followed by indoor chemical test analysis, which is complex and time consuming [1]–[3].

In recent years, the development of spectral monitoring techniques has provided new approaches for obtaining crop growth information. There are sensitive bands in the crop canopy reflectance spectra that are closely related to crop growth information; scientists can use the spectral characteristics of these sensitive bands to dynamically monitoring the crop growth indices and plant nutrient status [4]–[6]. In 1986, Shibayama *et al.* found that the vegetation index constructed based on the sensitive bands at 620 nm and 760 nm of rice reflectance spectrum had a strong correlation

The associate editor coordinating the review of this manuscript and approving it for publication was Muhammad Imran Tariq.

with leaf nitrogen content (LNC) and was less affected by rice variety [7]. In 2000, Tarpley *et al.* conducted the cluster analysis using multiple spectral ratios and found that the use of ratio of red edge band to short-wave near-infrared band to estimate the nitrogen nutrient status of crops could achieve high accuracy [8]. In 2010, Yao *et al.* constructed normalized difference spectral indices (NDSIs) and ratio spectral indices (RSIs) using the original wheat canopy hyperspectral data and its derivative value [9]. They found that NDSIs and RSIs could effectively indicate wheat leaf nitrogen accumulation. The prior body of research shows a certain relationship between the vegetation index of crop canopy and the content of crop nutrient elements. The acquisition of the crop canopy reflectance spectrum can be used to calculate the vegetation index, and then through the spectral monitoring model between the vegetation index and agronomic parameters, the accurate inversion of crop growth information can be realized.

Based on the identification technique that uses a characteristic spectrum, scientists over the world have developed some spectral monitoring apparatuses for crop growth. Depending on the light source used, this equipment can be divided into two categories, one is a passive device with sunlight as the light source, and the other is an active device with a light source of a specific band [10]–[14]. In 2004, Moya *et al.* designed a device to measure chlorophyll fluorescence that uses sunlight as the light source and successfully conducted measurements on a corn canopy. This experiment showed that the passive light source device used to measure chlorophyll fluorescence could achieve long-distance non-destructive vegetation measurement [15], [16]. In 2013, Zhong *et al.* designed a smart apparatus to detect crop nutrient condition, which used sunlight as the light source and could collect the sunlight radiation information and crop canopy reflective light information at wavebands of 550, 650, 766, and 850 nm and the spectral vegetation index was constructed. The experiments on winter wheat showed that the normalized vegetation index constructed at 550 nm and 760 nm could effectively predict the chlorophyll content of winter wheat [17]. Ni *et al.* developed a passive light source apparatus for crop growth monitoring and diagnosis. The monitoring and diagnosis apparatus could collect the solar radiation spectrum and crop reflectance spectrum information at the wavebands of 720 nm and 810 nm. Through the calculation of vegetation index and inverting of agronomic parameters, the real-time and non-destructive acquisition of growth indexes, such as crop Leaf nitrogen index (LNC) and leaf area index (LAI), could be realized [18], [19]. Field Spec series portable field spectrometers from Analytical Spectral Devices (ASD) Inc. (Malvern Panalytical, Malvern, Worcs, UK) use sunlight as the light source, and its wavelength detecting range is 350–2500 nm. The spectral sampling interval of 350–1000 nm is 1.4 nm, and the spectral resolution is 3 nm; the sampling interval of 1000–2500 nm is 2 nm, and the resolution is 10 nm; the field angle of the spectrometer probe is 250°. Due to their wide band range and high accuracy, they have been widely used in crop canopy spectral analysis [20], [21].

Compared with a passive light source device, an active light source device has its own light source, does not rely on solar light, can be used in all weather conditions, and is more suitable for obtaining crop growth information in different growth periods. In 2012, Osama Mohammed Ben Saeed *et al.* designed a portable four-band active light source sensor for measuring the ripeness of oil palm fresh fruit [11]. Narrow-band light-emitting diodes (LEDs) were used in the sensor as the light source, there were four spectral bands (570, 670, 750, and 870 nm), and this sensor could measure in all weather conditions. However, the existing application of the device is only for the measurement of the ripeness of oil palm fresh fruit, and the application range is limited [22]. In the GreenSeeker series of spectrometers developed by NTech Industries Inc. (USA), two independent red light (650 ± 10 nm) and near infrared light (770 ± 15 nm) LEDs are used to obtain normalized difference vegetation index (NDVI) and ratio vegetation index (RVI). The spectrometers have high measurement accuracy and produce good results, but they are expensive and there is a lack of agronomic parameter models. It cannot directly output agronomic parameters, cannot guide agricultural production, and is not conducive to promotion and commercialization [23], [24]. Cao *et al.* used the Crop Circle ACS-470 spectrometer developed by Holland Scientific to obtain the spectral reflectance of rice canopy. The instrument uses LED as the light source and can simultaneously collect the spectral reflectance information of three different bands. The vegetation index constructed by the reflectivity can successfully establish a relationship with the nitrogen content of rice [25]. The new-generation product RapidSCAN CS-45 from Holland Scientific Inc. also uses LEDs as the light source, can simultaneously obtain the spectral reflectance at the 670, 730, and 780 nm bands, and can construct the normalized difference red edge (NDRE) index. The instrument has a small size and simple structure, but it can only display NDRE parameters, has a single function, and cannot output crop physiological and biochemical parameters [26].

Compared with previous studies, contributions offered by this article can be summarized as follows:

1) An active light source apparatus for crop growth monitoring and diagnosis (CGMD) that is able to detect the growth information of wheat and rice crops under any weather or light conditions in a non-destructive, rapid, and efficient way was developed in this study. Some commercial devices, such as the GreenSeeker Handheld and RapidSCAN CS-45, also performed well during the testing, yet they are protected by intellectual property rights, expensive, and difficult for secondary development. In this study, the design idea, structure, key circuits, and software functions of the CGMD apparatus are described in detail, laying a good foundation for further studies.

2) In this study, a method for ambient light filtering was developed by integrating light source modulation and high-pass filters. By modulating the light source, the emergent light of the proposed instrument was controlled at a certain frequency to differentiate it from the ambient light. High-pass filters and other functional circuits were used to collect the characteristic spectrum and filter the spectral band in ambient light with the same characteristics. Field tests suggested that the influence of sunlight-dominant ambient light could be effectively eliminated by the proposed method.
3) The portable spectrometers currently on the market can only measure the spectral reflectance of the crop canopy and calculate the vegetation index, but they do not provide specific spectral monitoring models for real-time accurate prediction of crop growth parameters. Due to limited functions, they are not applicable to agricultural production in practice. In this study, a crop spectral monitoring model was built based on field tests on rice and wheat. The model, together with a fertilization diagnosis model, enabled the proposed instrument to output crop growth parameters and diagnosis results in a quick and intuitive way, making it more friendly to agricultural technicians than current instruments.

The remainder of this paper is organized as follows. Section II introduces the measuring principle of the CGMD apparatus and the selection of the characteristic wavelength band of the light source. The overall structure of CGMD apparatus as well as the structure and specific design of the built-in light source system and the light sensing system are presented in Section III. Section IV explains the design of the field experiments, the tested instruments, the test methods, Data analysis methods and results. Section V discusses the significance of this work and the problems that occurred in the experiment. In the end, section VI concludes this article.

II. MEASURING PRINCIPLE OF THE ACTIVE LIGHT SOURCE APPARATUS FOR CROP GROWTH MONITORING AND DIAGNOSIS

The different nitrogen nutrient elements in crops will cause changes in the spectral reflectance of the crop canopy at specific bands. As shown in **Fig. 1**, under different nitrogen fertilizer treatments, the spectral reflectance of the wheat canopy is significantly different between 460–730 nm and 760–1210 nm. Among them, the spectral reflectance of 460–730 nm exhibited a negative correlation with the amount of nitrogen fertilizer applied, the reflectance under N5 treatment was the lowest, and the reflectance under N1 treatment was the highest. The spectral reflectance from 760–1210 nm was positively correlated with the amount of nitrogen fertilizer applied, the highest and the lowest values were found under the N5 treatment and N1 treatment, respectively, and 710–760 nm was the distinct transition region.

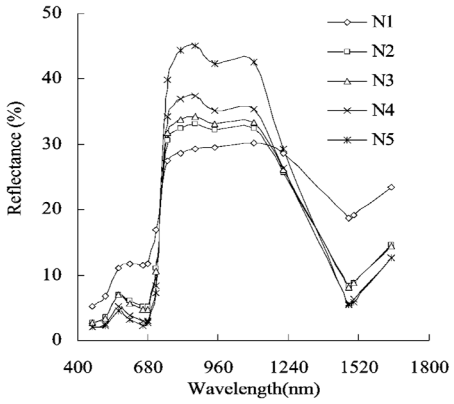

FIGURE 1. Multi-spectral reflectance of the wheat canopy under different nitrogen application levels (N1: 0 kg/hm^2, N2: 75 kg/hm^2, N3: 150 kg/hm^2, N4: 225 kg/hm^2, N5: 300 kg/hm^2) [27].

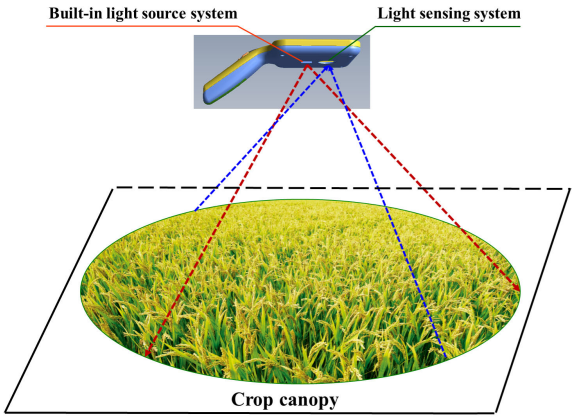

FIGURE 2. The measurement principle of the active light source apparatus for crop growth monitoring and diagnosis (CGMD).

Based on this principle, the proposed CGMD apparatus could generate emergent light at a certain band on crop canopy using the built-in light source system and receive the reflected light from crop canopy using the light sensing system. The vegetation index constructed by the spectral reflectance of a particular band was calculated by analyzing the spectral reflectance information, thereby performing effective extraction of crop growth information together with the spectral monitoring model. The test principle is shown in **Fig. 2**. According to existing research results, agronomic parameters such as LAI, LNA, and leaf dry weight (LDW) can characterize crop growth status well. The spectral reflectance values of a wheat canopy near 550 nm, 600–700 nm, and 720 nm will change as LNA changes. The spectral reflectance values of 580–700 nm and 770–900 nm exhibited a correlation with LDW. Meanwhile, the changes in the spectral reflectance around 460–680 nm and 810 nm had a high correlation with LAI [28]–[30]. Taking into account the sensitive bands of the three agronomic parameters, this paper selected the 730 nm and 810 nm bands as the characteristic bands to indicate the nitrogen content of rice and wheat.

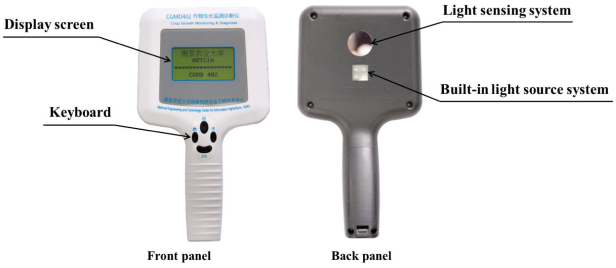

FIGURE 3. The overall structure of the CGMD apparatus.

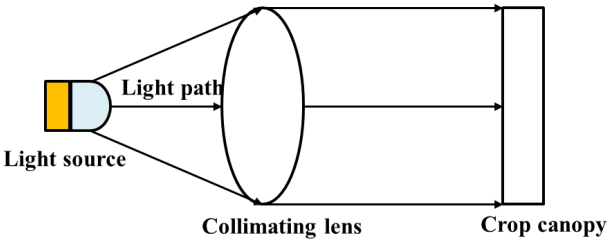

FIGURE 4. Structure of the built-in light source system.

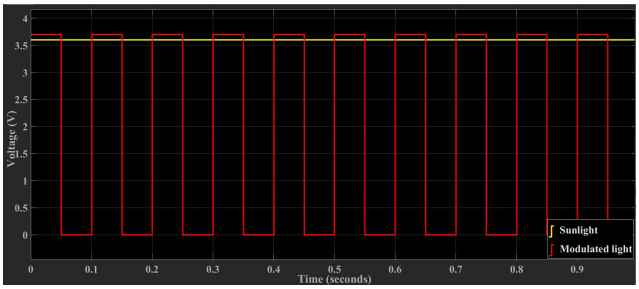

FIGURE 5. Waveform of sunlight and the modulated light source.

III. DESIGN OF ACTIVE LIGHT SOURCE APPARATUS FOR CROP GROWTH MONITORING AND DIAGNOSIS

Fig. 3 shows that the CGMD apparatus consists of the built-in light source system, light sensing system, and hardware circuits. It adopts the single-point static test mode, and the operator needs to stably hold the apparatus above the crop canopy to take a measurement. The operation and control of the CGMD apparatus are realized by mechanical keys, the test speed is very fast, and the whole process only takes 1–2 s.

A. DESIGN OF THE BUILT-IN LIGHT SOURCE SYSTEM

The built-in light source system consisted of the light source, emergent light path, and collimating lens. LED lights served as the light source. The irradiance of sunlight on the ground at noon on a clear day was taken as the reference. Two LED lights were used to provide luminescence at each spectral band to ensure spot intensity. Considering the small change in illumination intensity and the low changing frequency of sunlight in a short time, spectral modulation technology was used to modulate the spectral signal emitted by the LED light source within a certain frequency, thereby distinguishing the ambient light signal from the spectral signal of the proposed instrument. When the emergent light path of the built-in light source system was designed, factors such as the number and location of LED lights, power of LED light sources, and appropriate testing distance had been fully taken into account in order to accurately control spot intensity and ensure the proper intensity of the reflection spectrum. In terms of the design of the collimating lens, an elliptic spot that fitted the characteristics of crop cultivation and completely covered the crop canopy was determined by analyzing the variations in the canopy diameters of different crop varieties through the growth period. In addition, a light-shaping diffuser (LSD) film was used to ensure both the uniformity and the shape stability of the emergent light spot. The structure of the built-in light source system is shown in **Fig. 4**.

1) DESIGN OF THE LIGHT SOURCE

The light source of the CGMD apparatus can be an LED, laser, or xenon lamp. Among them, an LED light source has a small size and low heat dissipation requirements, and is low cost, easy to control, and better able to meet the design needs of portable apparatuses. In this paper, LED lights were selected as the light source. The half-value angle of the exiting light was about 10 degrees, and the radiation power was 45 mW.

Because ambient light, which is dominated by sunlight, also contains characteristic band information, when the LED light source is used directly for testing, the presence or absence of sunlight, sunlight intensity, and sunlight incidence angle changes will influence the test results. Sunlight has a stable light intensity in a short period of time, the frequency of light intensity changes is very small, and the frequency band is located in the low-frequency region. Through a spectral modulation technique, the spectral signals at the wavelengths of 730 nm and 810 nm emitted by the LED light source are modulated to a certain frequency, which can allow the light sensing system of the apparatus to differentiate the 730 nm and 810 nm spectral signals in sunlight and active light source by frequency. The modulation of the spectral signal refers to the process of changing one or several characteristic parameters of the optical carrier. By modulating the optical signal, it not only has the advantages of filtering out interference from the background signal and improving the signal-noise ratio, but also converts the direct current (DC) radiation signal to alternating current (AC) signal, which is more favorable for the communication and transmission as well as the anti-interference performance of spectral signals. The schematic diagram of the sunlight and modulated light waveforms is shown in **Fig. 5**.

2) DESIGN OF THE LIGHT PATH

Rice and wheat were the main test subjects for the CMGD apparatus, and they are row crops, meaning that they grow in continuous rows. An image of this type of crop has a soil and water layer background between the rows. To eliminate the

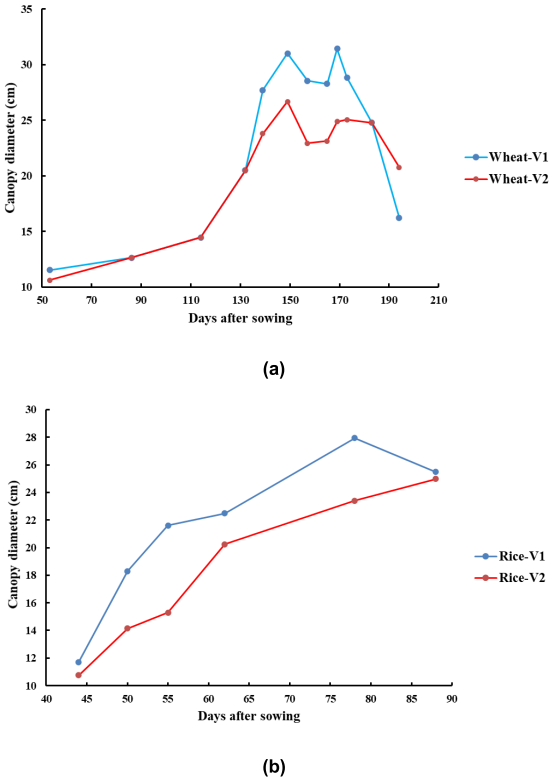

FIGURE 6. Changes in the canopy diameter of the rice and wheat cultivars. (a) Wheat (V1: Yangmai-12; V2: Aikang-14), (b). Rice (V1: Wuxiangjing-14; V2: Liangyoupei-9).

interference of the inter-row background on the test as much as possible, the light spot of the light source should meet the agronomic requirements of crop cultivation. We calculated the results of changes in the canopy diameter of the main rice and wheat varieties in Jiangsu, China with the growth period. To determine the light spot size, we measured changes in the canopy diameter of the main rice and wheat varieties in Jiangsu, China with the growth period, and the results are shown in **Fig. 6**.

Fig. 6 shows that the canopy width of wheat during the whole growing season ranged from 12–31 cm, and the canopy width of rice varied from 11–28 cm. In the early growth stage, the canopy diameter of rice and wheat is small, and the leaves are small and sparse, which cannot completely cover the field background between rows. When the light illuminates the background, it will easily affect the measurement. During the middle and late growth stages, the crop leaves become larger and denser; they can better occlude the background and reduce its impact during the test. To improve the test accuracy of the CGMD apparatus in the whole crop growth period, the lateral diameter of the light spot formed by the light source should be slightly less than the canopy width, and the longitudinal diameter of the light spot should cover at least two plants to reduce the effect of the individual plant difference on the measurement. Therefore, the minor axis length of the light spot was set to 10 cm, and the major axis length was set to 30 cm. The shape of the light spot is shown in **Fig. 7**.

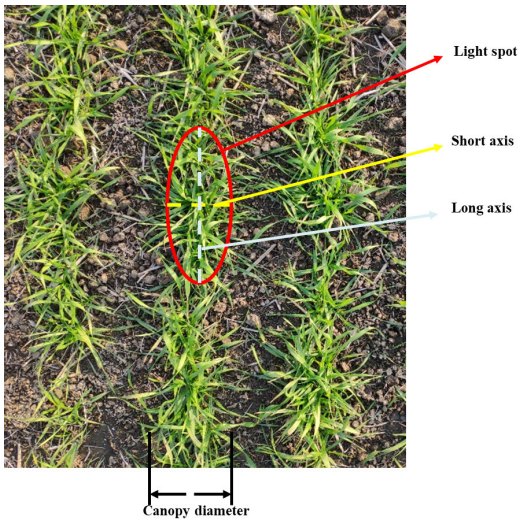

FIGURE 7. Shape of the light spot created by the built-in light source system.

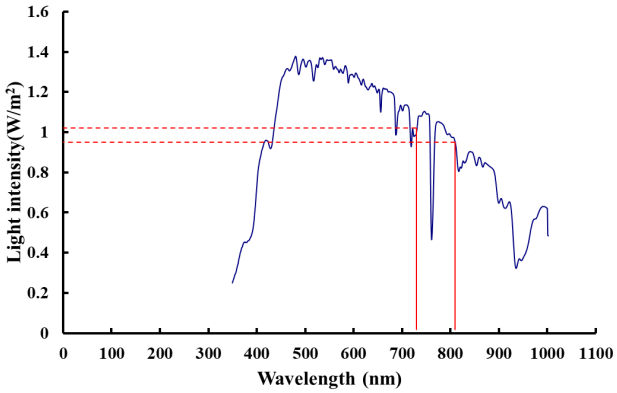

FIGURE 8. Distribution of solar irradiance.

After the light from the light source passes through the optical path system, an elliptical light spot needs to be formed. The illumination spot has a certain radiation intensity and is uniform and soft. Existing passive spectrometers, such as the ASD FieldSpec, which use sunlight as the light source, can stably measure spectral reflectance changes of the crop canopy. Thus, the solar radiation intensity can be used as an effective reference value for active light source instruments. Figure 8 shows the irradiance distribution of sunlight on the ground measured at noon on a clear day without clouds or fog with the CL-200F spectral luminance meter (Jingmai Instrument Inc., Henan, China). The results show that the irradiance of the sunlight at the 730 nm band was slightly larger than that at the 810 nm band and the intensity was about 1 W/m^2. In order to ensure that the crop canopy can generate a sufficiently strong reflectance spectral signal for subsequent processing, the irradiance of the light source to the crop canopy should be maintained at 1 W/m^2.

According to the selected LED parameters, the radiation power P was 45 mW, and the calculation of irradiance E is

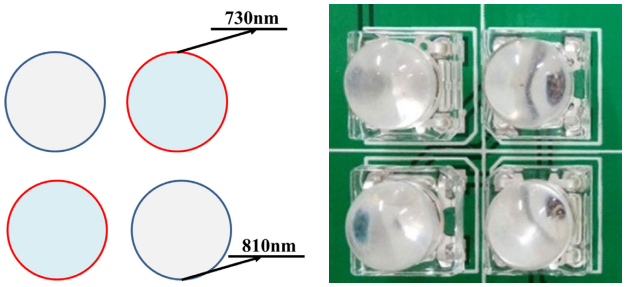

FIGURE 9. LED array distribution.

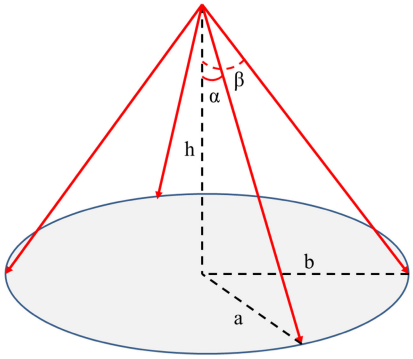

FIGURE 10. Diagram of the ellipse made by the emitted light.

shown in Equation (1),

$$E = \frac{dP}{dA} \tag{1}$$

where dA is the unit area of the illuminated surface and dP is the radiation flux received per unit area. The area of the ellipse formed from illumination spot can be calculated by Equation (2):

$$A = \pi^* a^* b \tag{2}$$

where A is the area of the ellipse, a is the semi-major axis length of the ellipse, and b is the semi-minor axis length of the ellipse.

According to the suitable measurement height of 60 cm (determined by the height and the test habits of the tester), a was 15 cm and b was 5 cm. After the values were substituted into the equation, the radiation intensity at a distance of 60 cm from the light source was calculated to be 0.478 W/m^2. Therefore, at least two LEDs were required as the light source for each of two wavelength bands of 730 nm and 810 nm. At the same time, in order to allow the light emitted by the LEDs in different wavelength bands coincide in the canopy and illuminate the same area, the LEDs were arranged in a crisscross pattern, as shown in **Fig. 9**.

When the above-mentioned LED array is used for light emission, the shape of the formed light spot is rectangular. However, the targeted shape should be elliptical, as shown in **Fig. 10**.

In this figure, h is the distance between the diffuser and the target surface, a is the short semi-axis of the illumination spot, b is the long semi-axis of the illumination spot, α is the angle of the exiting light in the direction of the short semi-axis, and β is the angle of the exiting light in the direction of the long semi-axis. The angle of exiting light, the spot size, and the height h satisfies the following relationship:

$$\tan\alpha = \frac{b}{h} \tag{3}$$

$$\tan\beta = \frac{a}{h} \tag{4}$$

The dimensions of the illumination spot were substituted into the equation (3) and (4), and the values of α and β were calculated to be 9.50° and 26.60°, respectively.

3) DESIGN OF THE COLLIMATING LENS

When using LED light sources to directly illuminate the crop canopy, the intensity of the rectangular spot formed was strong at the center and weak at the edges, and the light intensity distribution was uneven. Therefore, an optical collimation device, such as a cylindrical mirror or a diffuser, must be added in front of the LED, so that not only do the size and shape of the spot meet the design requirements, but also the irradiance is uniform throughout the spot. A cylindrical lens is an aspheric lens and is inexpensive, but it is large and heavy, so it is not suitable for the portability of the apparatus. A light shaping diffuser (LSD) is a micro-lens structure formed on the surface of the film by holographic technique. After the light passes through the film, the light diffuses uniformly according to the diffusion angle, and the formed illumination spot is softer and more uniform. Furthermore, LSDs are small and lightweight; therefore, an LSD diffuser was used for beam collimation.

According to the previous calculation of the light spot size, an LSD of 10° × 30° was selected. This study used Tracepro software (Lambda Research Corporation of Littleton, Massachusetts, USA) to model the built-in light source system. Tracepro is the first optical design and simulation software that uses the ACIS three-dimensional solid modeling kernel as the benchmark and possesses the functions of optical analysis, photometric analysis, and illumination system analysis. Furthermore, it can perform optical analysis in combination with actual solid models, has powerful functions, and is easy to operate. A test plate was placed at a distance of 60 cm from the LSD through Tracepro software to trace the light, and the irradiance distribution results were obtained by simulation, as shown in **Fig. 11**.

The results showed that the designed built-in light source system could obtain a 30 cm × 10 cm oval spot at a vertical distance of 60 cm, and the irradiance value was above 1 W/m^2. The uniformity of the spot was calculated to be 85% by using Equation (5) for calculating the illumination optical uniformity, and the requirements of spectral information collection were met.

$$U = \frac{E_{\max} - E_{\min}}{E_{\max} + E_{\min}} * 100\% \tag{5}$$

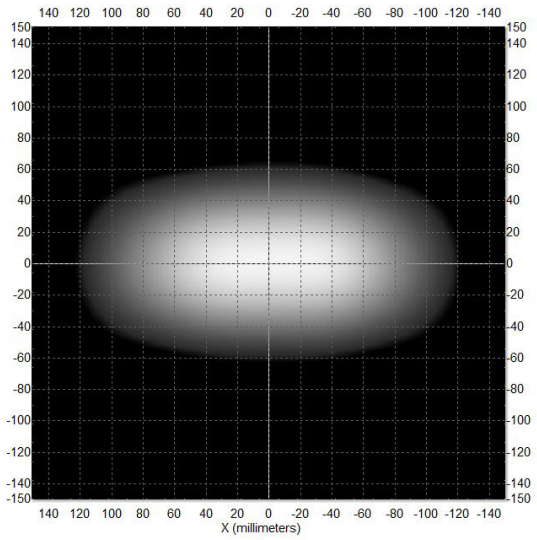

FIGURE 11. Irradiance distribution of the built-in light source system.

where U is the uniformity, Emax is the maximum value of the illumination spot intensity in the target area, and E_{min} is the minimum light intensity value of the illumination spot in the target area.

To verify the actual size and uniformity of the spot, the imaging results of the built-in light source system illuminating on a standard reflecting board in the darkroom were obtained using an industrial camera. The test platform is shown in **Fig. 12**; the light source is 60 cm away from the standard reflecting board (Size: 29.7 cm × 21 cm, Reflectivity: 80%).

The test results of the built-in light source system are presented in **Fig. 13**. To show the shape and size of the spot more clearly, the brightness of the original image was increased by 40%. The major axis of the spot was slightly larger than the length of the reflecting board while its minor axis was lightly smaller than the length of the reflecting board, i.e., the spot was an ellipse. After the invalid areas that had a low reflectance at the edge were removed, the size of the ellipse was about 28 cm × 12 cm, which was close to the simulation results. Spot uniformity was calculated using Equation (5) by reading the gray value shown by the standard reflecting board. The actual spot uniformity was about 95%, which was higher than the simulation results, indicating that the built-in light source system generally performed as intended.

B. DESIGN OF THE LIGHT SENSING SYSTEM

The function of the light sensing system is to receive the information of the crop canopy reflectance spectrum. The surface of the crop canopy can be approximately treated as a Lambertian surface [18]. After the LED light source illuminates to the crop canopy, diffuse reflection occurs. In order to ensure that the collected signal has sufficient strength, reduced light flux loss, and reduced noise interference, the light sensing system

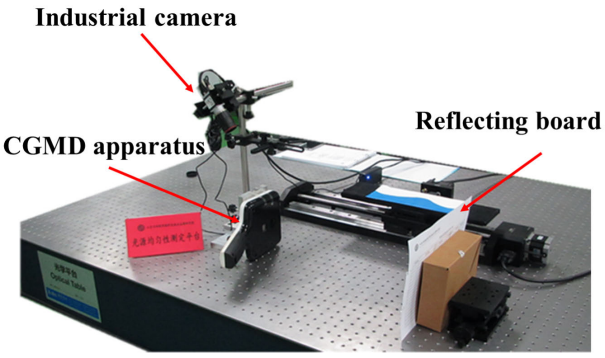

FIGURE 12. Optical test platform.

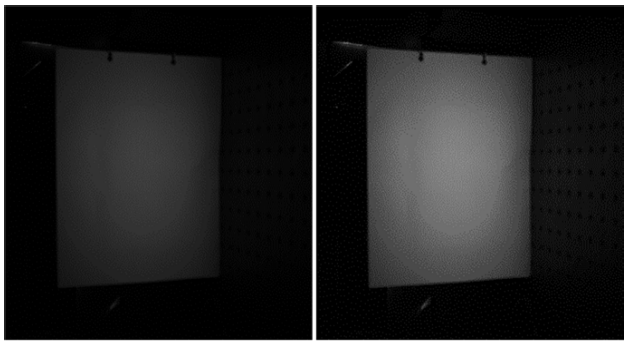

FIGURE 13. Test results of the lighting system.

consisted a photodetector and a condenser lens. **Fig. 14** is a schematic diagram of a light sensing system.

1) SELECTION OF THE PHOTOELECTRIC DETECTOR

Photodetectors mainly include photocells, photodiodes, phototransistors, and photoresistors. Compared with other photodetectors, photodiodes have the advantages of high sensitivity, short response time, wide spectral response, and wide range of test light intensity. The MID-A841 photodiode (Unity Opto Technology Co. Ltd., Taiwan, China) selected by this paper has high spectral responsivity at the 730 nm and 815 nm bands. The typical value of spectral responsivity is 0.18 (Amp/Watt)

2) DESIGN OF THE CONDENSER LENS

The function of the condenser lens is to collect the diffusely reflected light obtained after the light emitted by the built-in light source system is reflected by the crop canopy. The commonly used condenser lens is large and heavy, so it is not convenient for use in portable apparatuses. Fresnel lenses are prepared based on convex lenses, the parts that have no effect on the change in lens curvature are excavated, and only the parts that can show effective refraction are retained. Therefore, Fresnel lenses are small, lightweight, and easy to integrate.

Fresnel lens have a concentric ring structure, each ring zone retains the curvature characteristics of the original lens,

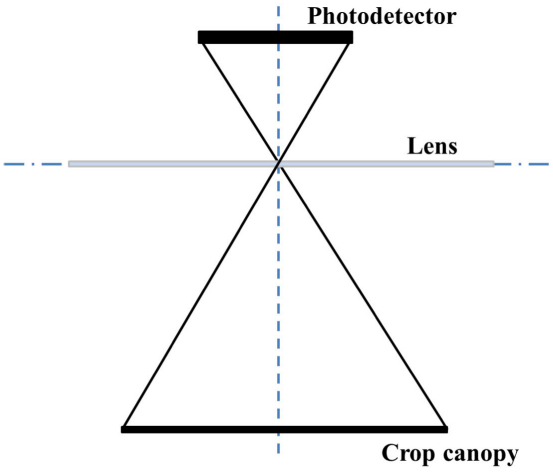

FIGURE 14. Schematic diagram of the light sensing system.

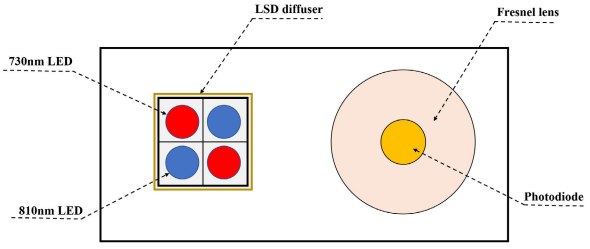

FIGURE 15. Schematic diagram of photodetector installation.

FIGURE 16. Photo of actual structure (asynchronous collection for the photodiode).

and the focusing performance is unchanged. The key of its design is to calculate the angle between the concentric grooves and the vertical direction by determining the focal length, thus completing the manufacturing process [31]–[33]. The light sensing system collects the crop canopy reflectance spectrum. In order to better obtain the condensing effect, the photodetector was located on the focal plane of the lens. During the assembly of the apparatus, in order to ensure that the thickness of the apparatus is not too large, the photodetector and the LED are soldered on the same circuit board with the same height, as shown in **Fig. 15** and **Fig. 16**.

For the Fresnel lens, its focus length was determined to be 15 mm by the apparatus size, its diameter was 30 mm, and its thickness was 2 mm. The design schematic diagram is shown in **Fig. 17**.

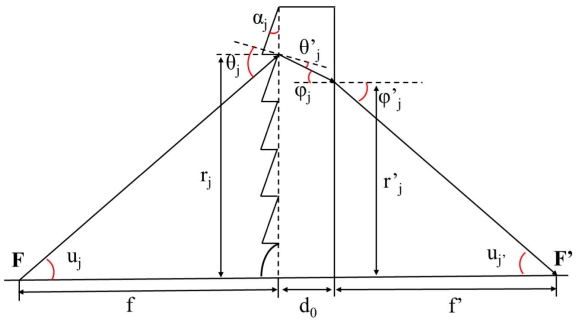

FIGURE 17. Schematic diagram of the flat Fresnel lens design.

In **Fig. 17**, F represents the left focal point of the Fresnel lens; F' represents the right focus of Fresnel lens; f and f' represent the left and right focal lengths, respectively; u_j is the angle between the incident light and the lens centerline, and u'_j is the angle between the exiting light and the lens center line angle; d_0 is the width of Fresnel lens; r_j is the distance from the incident point of the light to the lens centerline; r'_j is the distance from the exiting point of the light to the lens centerline; θ_j is the incident angle of the light, and θ'_j is the refraction angle of incident light; φ_j is the exiting angle, and φ'_j is the refraction angle of the exiting light; α_j is the angle between the concentric grooves and the vertical direction.

According to the knowledge of plane geometry,

$$\theta_j = \alpha_j + \mu_j, \alpha_j = \theta'_j, \varphi'_j = \mu'_j \tag{6}$$

$$\mathrm{tg}u_j = \frac{r_j}{f} \Rightarrow u_j = arctg\left(\frac{r_j}{f}\right) \tag{7}$$

The light entered on the surface of the ring zone of the lens, and the law of refraction gives:

$$\sin\theta_j = n\sin\theta'_j \tag{8}$$

The simultaneous equations (6), (7), and (8) could give:

$$\sin\left[\alpha_j + arc\left(\frac{r_j}{f}\right)\right] = n\sin\left(\alpha_j - \phi_j\right) \tag{9}$$

The following equation could be deduced from the figure:

$$tg\phi'_j = tgu'_j = \frac{r'_j}{f'} = \frac{r_j - d_0 tg\phi_j}{f'} \tag{10}$$

The light exited the lens surface, and the law of light refraction could give:

$$\mathrm{n}\sin\phi_j = \sin\phi'_j \tag{11}$$

The simultaneous equations (9), (10), and (11) give:

$$n\sin\left\{\alpha_j - \arcsin\left(\frac{1}{n}\sin\left[\alpha_j + arc(\frac{r_j}{f})\right]\right)\right\}$$
$$= \sin\left\{arctg\left(\frac{r_j - d_0 tg\left\{\alpha_j - \arcsin(\frac{1}{n}\sin[\alpha_j + arctg(\frac{r_j}{f})])\right\}}{f'}\right)\right\} \tag{12}$$

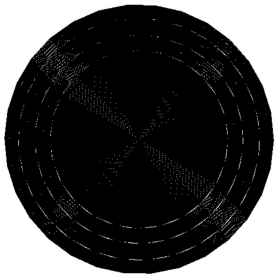

FIGURE 18. Fresnel lens model.

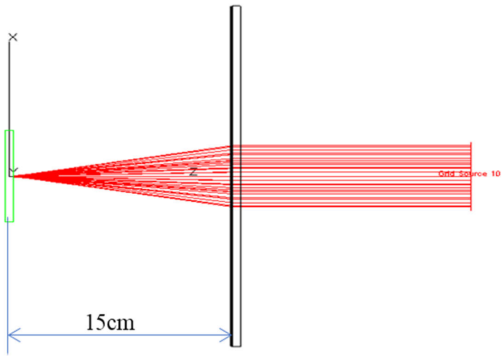

FIGURE 19. Schematic diagram of ray tracing of parallel light source through Fresnel lens.

According to the settings, $n = 1.5$, $r_j = 15$ mm, $f = 15$ mm, $f' = -15$ mm, and $d_0 = 2$ mm were substituted into the equation, and the angle α_j between the concentric grooves and the vertical direction was calculated to be 7.80°.

In order to verify the performance of the designed Fresnel lens, the Fresnel lens parameter values were input into the optical simulation software Tracepro, and a Fresnel lens model was established, as shown in **Fig. 18**. A parallel light source was set in Tracepro and vertically illuminated the Fresnel lens. The ray tracing result is shown in **Fig. 19**: The parallel beams passed the Fresnel lens and were focused on a point 15 mm from the lens. The Fresnel lens met the design requirements.

C. HARDWARE CIRCUIT

The hardware circuit of the monitoring and diagnosis apparatus mainly included a signal conditioning circuit module, an ATmega32 microprocessor, a constant-current source drive module, a temperature and humidity sensor module, a keyboard input module, and a liquid crystal display (LCD) module. Among them, the signal conditioning circuit module was used to collect and process the information of crop-canopy reflectance spectrum. According to the analog-digital convert ability of the selected microprocessor, the test resolution of the instrument is about 0.001. The constant-current source drive module was used to control the time-sharing lighting up of LED light source. The microprocessor module was used to realize the spectral vegetation index calculation, model coupling, and inverting

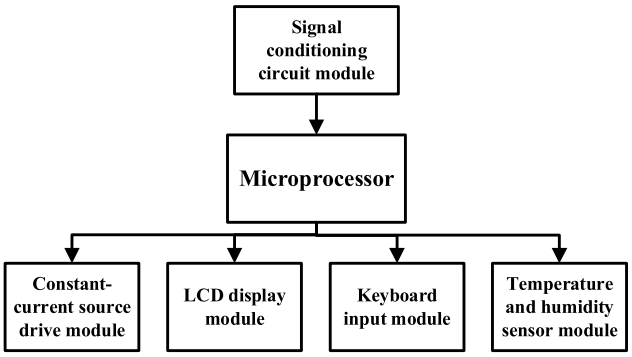

FIGURE 20. Overall design of the hardware circuit.

of agronomic parameters. The keyboard input module was used for switching the instrument function interface and user input. The liquid crystal display module was used to display real-time measurement results and diagnosis results. The hardware circuit structure of the CGMD apparatus is shown in **Fig. 20**.

1) DESIGN OF THE SIGNAL CONDITIONING CIRCUIT

The signal conditioning circuit was used to perform photoelectric conversion, filtering, shaping, and appropriate amplification of the reflectance spectral signal output by the photodetector; it mainly included an I-V conversion circuit, a high-pass filter circuit, and a peak detection circuit. In order to identify the modulated light generated by the constant-current drive module, a high-pass filter was used to extract the signal and filter out the low-frequency solar spectrum signal after the current-voltage conversion was realized on the I-V conversion circuit. However, the effective signal extracted by this circuit also contained high-frequency electromagnetic noise. Therefore, after the high-pass filter, a multiple feedback active band pass filter with a center frequency of 1 kHz was used as a peak detection circuit to filter the high-frequency noise. In addition, the multiple feedback band-pass filters and the inverting proportional adder were combined, and the resistance parameters were adjusted, enabling the circuit to fulfill voltage conversion, and filtering simultaneously. The waveform of the output volage was shifted above the time axis. Thus, the circuit had a strong anti-interference capacity.

2) DESIGN OF THE CONSTANT-CURRENT DRIVE MODULE

LED has similar volt-ampere characteristics as the diode. The light intensity is proportional to the forward current. In order to ensure the stability of the light intensity, the DD312 constant current source chip (Dianjing Technology Co., Ltd., Taiwan, China) is selected to drive the LED because of its high precision and high integration. The chip can also accept a control signal with a maximum frequency of 1KHz to realize the light source modulation function. In the field testing of the CGMD apparatus, a large difference was observed on ambient light between sunny day and cloudy day conditions. In order to eliminate the influence of ambient light, the

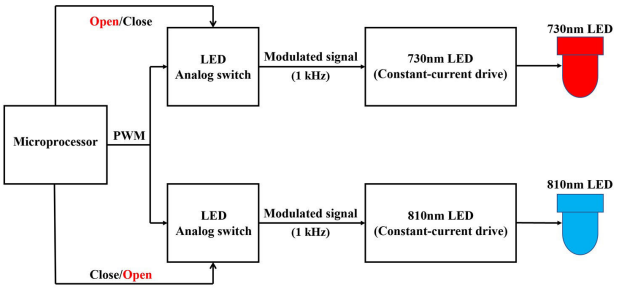

FIGURE 21. Schematic diagram of modulation signal generation.

frequency modulation signal was used to control the LED light source to emit modulated light with a frequency of 1 kHz. Compared with sunlight, this modulated light had a high frequency and could be effectively extracted by a filter circuit. The LED light source modulation signal was generated by the pulse width modulation (PWM) module of the microprocessor, and was output to the analog switch through the I/O port to control the lighting up LEDs at the 730 nm and 810 nm bands. In a short period of time, the physiological state and spatial distribution of crop canopy did not change greatly. Therefore, time-sharing lighting was used to obtain the reflectance spectrum values of the two bands of the crop canopy. The power consumption in the time-sharing mode was only half of that when LEDs were on continuously, which greatly reduces the power consumption of the system. The modulated signal generation diagram is shown in **Fig. 21**.

3) DESIGN OF THE SOFTWARE SYSTEM

The software system consisted of three modules: program initialization, I/O interface resource control, and the application program. The program initialization module was used for microprocessor self-test and initialization, keyboard input module, and LCD initialization. The I/O interface resource-control module was used to control the key-pressing measurement, function switching, LED lighting control, and LCD display. The application program module was used for collecting the information of crop canopy reflectance spectrum, preprocessing spectral information, calculating crop canopy reflectance, and coupling vegetation index with crop growth model. The entire software system adopted the modular design, which was easy to debug, transfer, and upgrade.

The CGMD apparatus was equipped with three function keys: measurement, monitoring, and diagnosis. In the measurement mode, the microprocessor generated PWM signals that were output to the analog switch through the I/O interface. It controlled the time-sharing lighting up of LEDs at 730 nm and 810 nm. The exiting light illuminated on the crop canopy, and the photodetector received the reflectance spectrum information simultaneously. In monitoring mode, the microprocessor calculated the measured canopy spectral reflectance value, RVI value, and NDVI value, was coupled with crop growth monitoring model to invert growth indices, such as LNA, LDW, and LAI, and displayed them on the LCD. In diagnostics mode, the user could input the

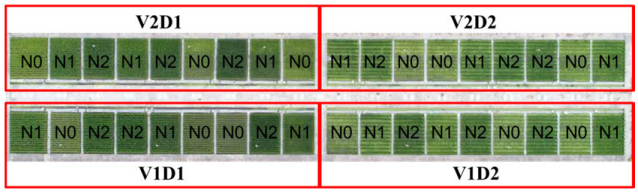

FIGURE 22. Aerial photograph of the wheat experiment setup.

nutrient index model parameters, including target yield of the test area, amount of nitrogen absorbed by 100 kilograms of grains, and RVI value of high-yield areas through the keyboard to diagnose the fertilization situation at the current test site [34], [35]. The diagnosis results were displayed on the LCD in real time.

IV. EXPERIMENT AND ANALYSIS OF RESULTS

A. DESIGN OF FIELD EXPERIMENT

The designed wheat field experiments were conducted at Rugao base in Nantong City, Jiangsu Province from March to May 2017. Two wheat varieties, i.e., V1 (Ningmai-13), and V2 (Huaimai-33) were set up in the experimental field. Three nitrogen fertilizer levels—N0 (0), N1 (180 kg/hm2), and N2 (270 kg/hm2)—were selected, the ratio of base fertilizer to top dressing is 5:5, and two planting row spacings, i.e., D1 (25 cm) and D2 (40 cm) were used. Three repetitions were conducted, and there were a total of 36 plots, each with an area of 5 m × 6 m. Each plot is planted independently and did not interfere with each other. In addition, phosphate fertilizer was applied at a rate of 120 kg/hm^2, potassium fertilizer was applied at a rate of 135 kg/hm^2, and both fertilizers were applied one time along with the base fertilizer. The remaining field management measurements were carried out by professional agricultural technicians. The aerial photograph of the experiment setup is shown in **Fig. 22**.

The designed rice field experiments were also conducted at Rugao base in Nantong City, Jiangsu Province from July to September 2017. The experimental varieties were V1 (Huaidao-5) and V2 (Wuyunjing-27). The nitrogen fertilizer levels used were N0 (0), N1 (180 kg/hm2), and N2 (360 kg/hm2), the ratio of base fertilizer to top dressing is 4:6. The planting row spacings selected were D1 (30 cm) and D2 (50 cm). Three repetitions were conducted, and there was a total of 36 plots, each with an area of 5 m × 6 m. Each plot is planted independently and does not interfere with each other. The phosphate and potassium fertilizer application rates were the same as those used in the wheat experiment. The remaining field management measures were carried out by professional agricultural technicians.

B. EXPERIMENTAL EQUIPMENT

1) ACTIVE LIGHT SOURCE APPARATUS FOR CROP GROWTH MONITORING AND DIAGNOSIS

The hardware system of the CGMD apparatus designed in this paper was assembled, and the software program was

downloaded to complete the overall assembling of the monitoring and diagnosis apparatus to conduct field experiments.

2) ASD HANDHELD 2 FIELD SPECTROMETER

The ASD FieldSpec HandHeld 2 spectrometer (Malvern Panalytical, Malvern, Worcs, UK) can be used for the reflection-spectrum acquisition of different objects such as crops, marine organisms, and minerals. The device has the advantages of portability, simple operation, and accurate results. It has a test wavelength range of 325–1075 nm, wavelength accuracy of ± 1 nm, spectral resolution of less than 3 nm, and test field-of-view is 25°.

3) LAI-2200C PLANT CANOPY ANALYZER

The LAI-2200C plant canopy analyzer (LI-COR Biosciences, Lincoln, NE, USA) uses a ''fisheye'' optical sensor (vertical field-of-view, 148°; horizontal field-of-view, 360°) to measure the transmitted light at five angles above and below the vegetation canopy, and uses the radiation transfer model of the vegetation canopy to calculate the canopy structure parameters, such as LAI, mean leaf inclination angle, void ratio, and aggregation index. The LAI-2200C is based on the mature LAI-2000 technique platform and has a built-in GPS module. It can integrate GPS information and perform scattered light correction, making the LAI-2200C suitable for the measurement under any weather conditions.

C. MEASUREMENT METHOD

1) VERIFICATION OF THE INFLUENCE OF AMBIENT LIGHT ON APPARATUS PERFORMANCE

The tests were carried out in 12 planting areas with different nitrogen treatments (N0, N1, and N2), varieties (V1 and V2), and planting densities (D1 and D2) on clear and cloudless days during the tillering stage, the stem elongation, and the booting stage of wheat. One measurement point was randomly selected and located in each planting area. Each point was measured for three times, with the mean taken as the measured value. Based on the change in solar altitude, the CGMD apparatus was used to measure the NDVI and the RVI of the wheat canopy at the same location in each planting area at 10:00 a.m., 13:00, and 16:00 in the afternoon. The instrument was mounted in a fixed position 60 cm above the canopy, which was determined using a measuring tape. Whether ambient light intensity would impact the performance of the proposed instrument was identified by comparing and analyzing the test results.

2) COMPARISON OF MEASUREMENTS TAKEN AT DIFFERENT HEIGHTS

The tests were performed during the tillering stage, stem elongation, and booting stage of wheat and rice. The CGMD apparatus was held by hand at 40, 50, 60, and 70 cm (determined using the measuring tape) above crop canopy to obtain the NDVI and RVI results of the crop canopy in 12 planting areas with different nitrogen treatments (N0, N1 and N2), varieties (V1 and V2), and planting densities (D1 and D2). One measuring point was determined in each planting area. Each point was measured three times, with the mean taken as the measured value. Instrument stability at different heights was validated by comparing and analyzing the test results.

3) SPECTRAL DATA MEASUREMENT OF DIFFERENT INSTRUMENTS

Crop canopy spectra of different nitrogen application levels in different growth periods (tillering, stem elongation, and booting) of the two crops were measured using the CGMD apparatus. The NDVI and RVI results of total 36 planting areas were obtained. Each planting area was measured at three different points. Each point was measured for three times, with the mean taken as the measured value. Finally, a total number of 144 results were collected. The ASD FieldSpec HandHeld 2 portable spectrometer, widely recognized commercial instrument for crop spectrum monitoring [15], was used to measure the characteristic spectral reflectance and reflection spectrum of crop canopy simultaneously during the tests. NDVI and RVI results were calculated based on the characteristic spectral reflectance. Three different points at each planting area was measured; each point was measured three times. Measurement results were then compared and analyzed.

4) DETERMINATION OF AGRONOMIC PARAMETERS

The agronomic experiment and the spectroscopic apparatus test were carried out simultaneously. The wheat sampling method was to collect 20 single stems of each plot, and the organs were separated indoors. The rice sampling method was to select representative three holes for each plot. After sampling, according to the development of plant organs, the sample plants were separated into leaves, stem sheaths, and ears, and the LAI-2200C plant canopy analyzer was used to measure the leaf area index of each plot. The obtained samples were fixed at 105°C for 30 min and baked at 80°C to constant weight, followed by weighing, and then the dry matter mass of each organ per unit field area was calculated. After the sample was crushed, the LNC was determined by the Kjeldahl method.

D. DATA ANALYSIS

For the ambient light influence verification test and the comparison test of different heights of the CGMD apparatus, the standard deviation, and the coefficient of variation (CV) were used to evaluate the stability of the results. For the vegetation index test results and agronomic parameter results of the CGMD apparatus, the spectral monitoring models based on the correlation spectral vegetation index were established through linear and nonlinear regression analysis. The model was comprehensively evaluated using the coefficient of determination (R2), root mean square error (RMSE), and ratio of performance to deviation (RPD).

The RPD was calculated as follows:

$$RPD = \frac{Sd}{SEP} \tag{13}$$

where Sd is the standard deviation of the sample, and SEP is the standard error of prediction.

When RPD $<$ 1.4, the model prediction effect is poor; when 1.4 $\leq$ RPD $<$ 2, the model is better and can be used for result prediction; when 2.0 $\leq$ RPD $<$ 2.5, the model prediction accuracy is high and can be used for quantitative prediction [36].

E. RESULTS

1) TEST RESULTS OF THE INFLUENCE OF AMBIENT LIGHT ON INSTRUMENT PERFORMANCE

The NDVI and RVI results of crop canopy measured by CGMD apparatus at different measuring times during different growth periods of wheat are shown in **Fig. 23**; as shown, CGMD apparatus had consistent test results at different test times on the same test day. A high discrimination between planting areas with different nitrogen treatments was also observed. At different test times, the maximum standard deviation of NDVI was 0.027 and the maximum CV was 9.03%; the maximum standard deviation of RVI was 0.126 and CV was 6.04%. Moreover, the proposed instrument appeared with high stability under the sunlight of different intensities and was able to overcome the interference of ambient light with test performance.

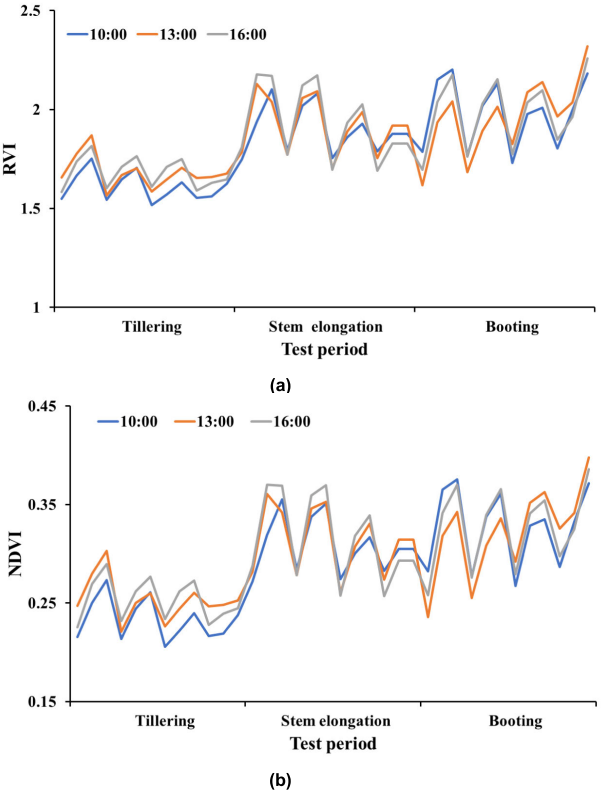

FIGURE 23. Comparison between the test results of CGMD apparatus at different time points. (a). RVI results. (b). NDVI results.

2) TEST RESULTS OF THE INFLUENCE OF HEIGHT ON INSTRUMENT PERFORMANCE

The NDVI results obtained by CGMD apparatus at different heights above the wheat and rice canopies are shown in **Fig. 24**. According to the results of wheat, the test results at the height of 70 cm during the booting stage of wheat fluctuated. By contrast, the test results obtained at various heights during the rest two stages showed little difference and changed consistently. The maximum standard deviation of different test results was 0.05; the maximum CV was 16.6%. When the test results at the height of 70 cm were excluded, the maximum standard deviation dropped by 0.023 and the maximum CV by 8.03%. As for the test results of rice, there was noticeable difference between the test results at the height of 70 cm and those at the other heights in all growth periods tested, especially the tillering stage. Such difference diminished during the stem elongation and the booting stage. The standard deviation of the test results was 0.054; the maximum CV was 18.3%. When the test results at the height of 70 cm were eliminated, the maximum standard deviation declined by 0.023 and the maximum CV declined by 6.99%. It can thus be inferred that the proposed instrument had a high stability within the given range of height. However, it performed unstably when the test height exceeded that range, which was particularly significant in the case of rice.

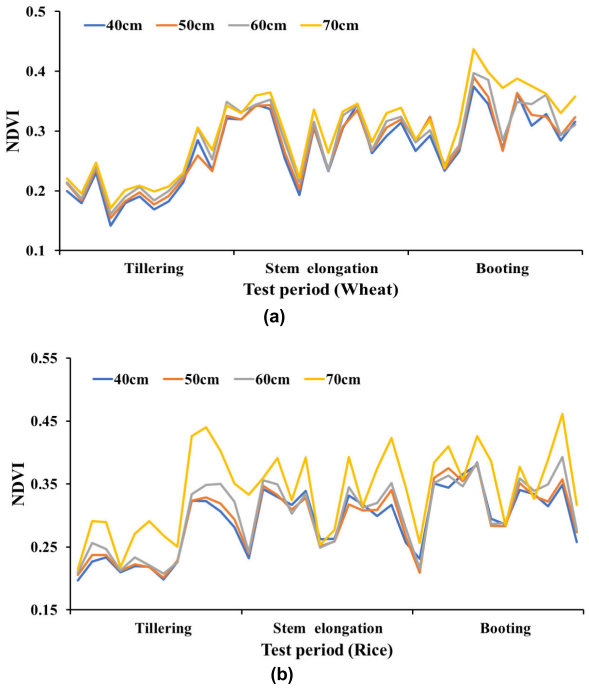

FIGURE 24. NDVI results measured using CGMD apparatus at different heights above the wheat and rice canopies. (a). Wheat. (b). Rice.

3) TEST RESULTS OF THE CONSISTENCY BETWEEN DIFFERENT INSTRUMENTS

To verify the measurement accuracy of CGMD apparatus, the commercial ASD Fieldspec HandHeld2 spectrometer was used for synchronous testing. The NDVI and RVI obtained from the same spectral band test were used for linear regression analysis. CGMD apparatus is pre-written with a vegetation index calculation model, which can directly output NDVI

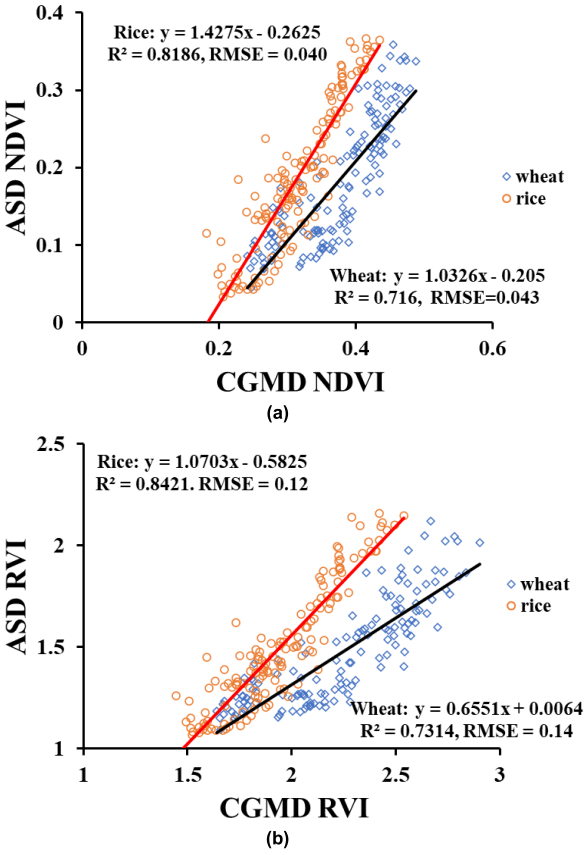

FIGURE 25. NDVI results measured using CGMD apparatus at different heights above the wheat and rice canopies. (a). Wheat. (b). Rice.

and RVI. The vegetation index results of ASD Fieldspec HandHeld 2 were calculated by extracting the reflectance of the corresponding spectral band. The results are shown in **Fig. 25**.

According to the results in **Fig. 25**, the determination coefficient (R^2) values of NDVI and RVI obtained by the two instruments for wheat test were 0.716 and 0.7314, respectively, and the RMSE were 0.043 and 0.14, respectively. Similarly, for rice, the R^2 values of NDVI and RVI obtained by the two instruments were 0.8186 and 0.8421, respectively, and the RMSE were 0.40 and 0.12, respectively. The test results between CGMD apparatus and ASD for rice and wheat have high consistency. The CGMD apparatus designed in this paper can accurately obtain the canopy vegetation index of rice and wheat.

4) ESTABLISHMENT OF THE SPECTRAL MONITORING MODEL

In the spectral model building test, regression analysis of the NDVI and RVI results (obtained using CGMD apparatus), the LAI (obtained using LAI-2200C) and the LDW, LNC, and LNA (obtained by the agronomic test) in all growth periods of wheat and rice was made. The spectral monitoring model for the relationship between vegetation index and agronomic parameters was built and written into the proposed instrument to realize the real-time inversion of agronomic parameters (**Fig. 26**).

As shown in **Fig. 26**, the relationship between the NDVI measured by CGMD apparatus and the LAI of wheat was more in line with the exponential model variation. Therefore, regression analysis of these two parameters was made using the exponential model, whereas the models for the relations between the other agronomic parameters and vegetation index were built by means of linear regression. According to the regression results, the R^2 values of the fitting between NDVI and the LAI, LDW, LNC, and LNA of wheat measured by the CGMD apparatus were 0.7877, 0.673, 0.6105, and 0.6647, respectively; the respective RMSEs were 0.86, 59.90, 0.76 and 2.87. By contrast, the R^2 values of the fitting between RVI and the agronomic parameters of wheat (LAI, LDW, LNC, and LNA) were 0.7881, 0.6944, 0.5973, and 0.6818, respectively; the respective RMSEs were 0.86, 51.87, 0.78, and 2.80. For rice, the R^2 values of the fitting between NDVI and LAI, LDW, LNC, and LNA were 0.7098, 0.6742, 0.3835 and 0.7247, respectively; the respective RMSEs were 1.18, 65.85, 0.25 and 2.73. In comparison, the R^2 values of the fitting between RVI and the agronomic parameters of rice (LAI, LDW, LNC, and LNA) were 0.6908, 0.6787, 0.3766, and 0.7489, respectively; the respective RMSEs were 1.25, 66.06, 0.25 and 2.60. It can be seen from the RPD calculation results that the RPD values of the prediction models for the LAI, LDW, and LNA of wheat and rice built based on the NDVI and RVI measured by the CFMD402 were larger than 1.4, indicating that the models performed favorably in prediction. In addition, the RPD of the prediction model for wheat LNC was also about 1.4, which suggested that it could be used for wheat LNC prediction. However, the RPD of the prediction model for rice LNC was small. Specifically, the RPD values the model for rice LNC predicted by NDVI and RVI were as small as 1.06 and 1.08, respectively, which demonstrated that the model for rice prediction performed poorly.

V. DISCUSSION

According to the results on the non-destructive acquisition of reflection spectrum in this study, crop growth information could be acquired using the proposed method in a rapid, real-time, and non-destructive way. Monitoring crop growth using ground spectrometers has also become a major means of agricultural information acquisition. Compared with vehicle-mounted spectrometers and remote sensing spectrometers, handheld ground object spectrometers are smaller, lighter, and easier to use. They are available on demand and can provide field management with decision-making information in real time. So far, instruments, such as ASD FieldSpec, Greenseeker, and Rapid Scan, have been applied in practice and obtained favorable results [37]–[40]. However, these instruments are mostly designed for commercial purposes. Intellectual property protection has not only pushed up the prices but also made it hard for secondary development based on these products due to non-public

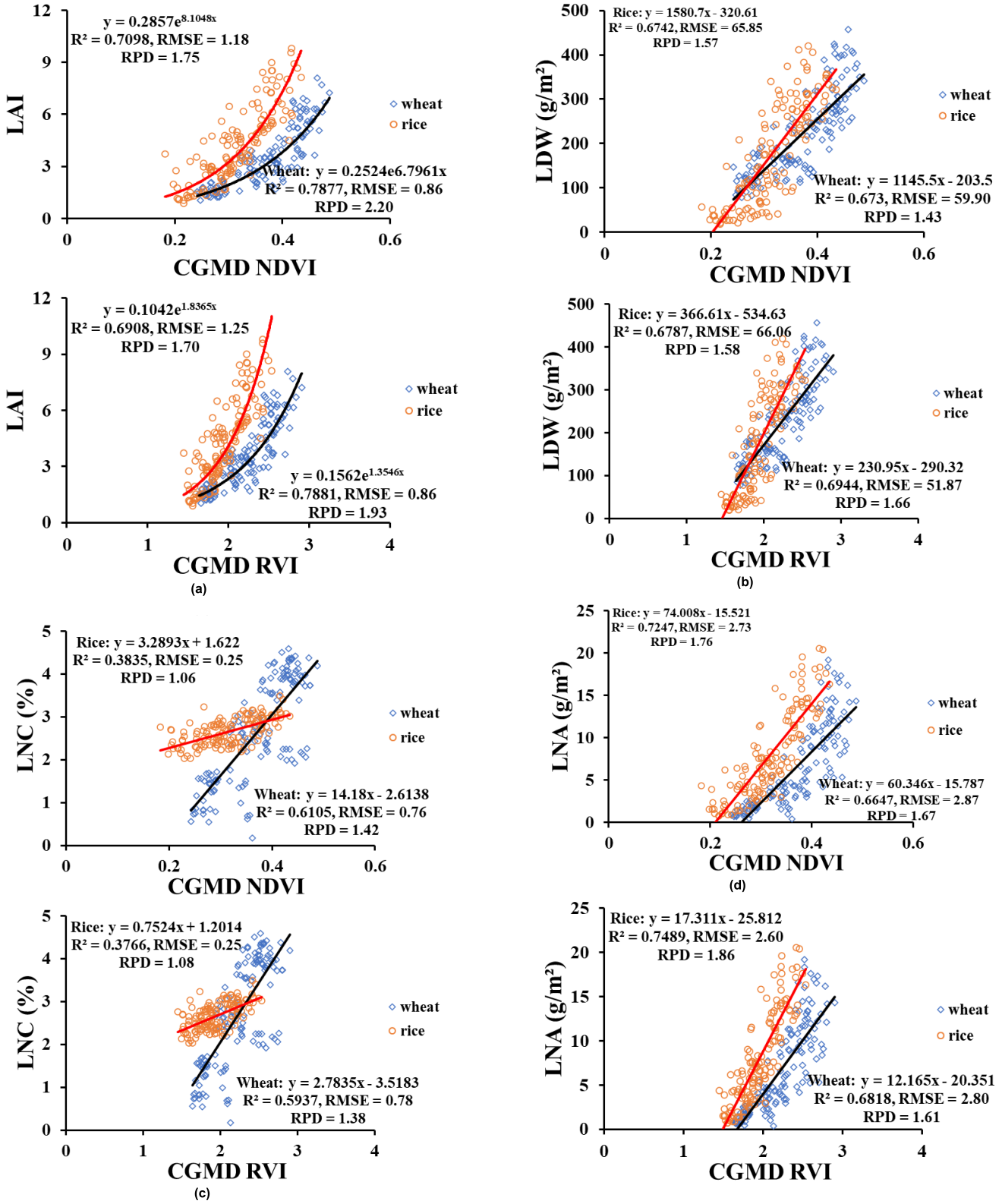

FIGURE 26. Establishment of the spectral monitoring model based on CGMD apparatus. (a). LAI prediction model. (b). LDW prediction model. (c). LNC prediction model. (d). LNA prediction model.

technical details. In addition, the indicators these commercial spectrometers measure are spectral reflectance and vegetation index, and they cannot present the agronomic parameters of crops and nitrogen nutrition diagnosis results in real time

for lack of accurate spectral monitoring models. For these reasons, an active light source apparatus for crop growth monitoring and diagnosis was developed in this study by analyzing the cultivation characteristics of row crops based on the long-term experience in wheat and rice reflectance spectrum test. More importantly, all the technical details regarding the proposed instrument have been made public, including the design idea, instrument structure, main software and hardware functions, and test methods. To better promote it among agricultural technicians and apply it to agricultural production, the tests on wheat and rice with different nitrogen treatments were designed to develop a crop canopy spectral monitoring model for real-time acquisition and direct display of wheat and rice growth parameters. Apart from the test results mentioned in this study, agronomic tests were continued to optimize the model, improve model performance, enhance test accuracy, and strengthen model universality after the proposed instrument was developed.

Spot size design was simulated using Tracepro and validated by tests. There was slight difference between the measured spot size and simulation result, but it basically complied with the design requirements. Also, the spot uniformity was superior to the simulation result. To test the actual performance of the proposed instrument, the ambient light influence test and the height comparison test were designed and conducted. According to the results of the ambient light influence test, the proposed instrument was less affected by ambient light and showed high stability at different times. The maximum CV of NDVI and RVI were as small as 9.03% and 6.04%, respectively. In the test on the influence of height, the proposed instrument worked stably in wheat and rice testing within the standard test height of 60 cm. It fluctuated little in wheat testing when the test height reached over the standard range, but greater fluctuations were observed in rice testing throughout all growth periods. One possible reason was that the spots generated by the built-in light source system were smaller and the radiation intensity of the spot per unit area was stronger when the test height was less than 60 cm. In this case, the spots could still cover crop canopy well in all growth periods. However, the spot area was larger than the designed standard area when test height was over 60 cm, which made it easier for light to spread to the field from the edge of crop canopy. Considering that the reflection of water layer is much stronger than that of soil, the test result was more susceptible to interference.

The spectral model building test suggested that NDVI and RVI obtained by CGMD apparatus performed poorly in predicting the LNC of rice. Specifically, the RPD values were only 1.06 and 1.08, respectively. There was difference in the rest of the agronomic parameters of rice between the planting areas with low and high nitrogen treatments, but LNC did not show this type of difference. A possible explanation was that the problems that arose during the indoor tests and analysis had resulted in poor data discrimination, which will be validated in subsequent tests.

VI. CONCLUSION

1) In this study, a double-band active light source apparatus for crop growth monitoring and diagnosis was developed. A method to filter the interference signal of ambient light while collecting the valid reflection signal from the light source by means of light source modulation and high-pass filtering was put forward. High-frequency electromagnetic noise was further filtered using active band-pass filters, thereby enhancing the signal-noise ratio and the measurement accuracy of the instrument. Also, the built-in light source system that is able to generate uniform elliptic spots at the vertical height of 60 cm was designed based on the cultivation characteristics of wheat and rice. According to the Lambertian reflection characteristics of a crop canopy, a Fresnel lens with a focal length of 15 mm, diameter of 30 mm, thickness of 2 mm, and an angle of 7.8° between the sawtooth and the vertical direction was designed to collect the diffuse reflection light from crop canopy.
2) Both the built-in light source system and the light sensing system were designed based on single-point statistic test using the CGMD apparatus. Therefore, there is still room for improvement in the test method. After building the high-accuracy spectral monitoring model, the luminescent property and effect of light source in the dynamic environment would be analyzed, based on which the built-in light source system and the light sensing system that are capable of dynamic monitoring can be designed. Additionally, functions like handheld scanning, vehicle-mounted testing, and low-altitude remote sensing testing can be added to strengthen instrument performance, diversify its monitoring methods, and satisfy the test demands of different users and field scales.
3) According to the vegetation indices of wheat canopy obtained at different times within one test day, the combination of light source modulation and the filter circuit can favorably isolate ambient light; the results tested at different times are stable with small standard deviations and variation coefficients. The test results obtained at different heights suggest that the proposed instrument works stably within the prescribed range of height. When the test was conducted at a larger height, large fluctuations in the test results were obtained and significant increases in standard deviation and CV were observed. It indicates that it is necessary to take the applicable height range of the instrument into full consideration when designing the light source of the active light source spectrometer.
4) The results of wheat and rice throughout the growth periods indicated that the spectral monitoring model built in this study perform well in predicting the LAI, LDW, and LNA of wheat and rice. The RPD values were larger than 1.4 in all cases. To summarize,

the spectral monitoring model built based on this agronomic test allows real-time, quick, and accurate acquisition of wheat and rice growth information.

REFERENCES

[1] M. S. Moran, Y. Inoue, and E. M. Barnes, "Opportunities and limitations for image-based remote sensing in precision crop management," *Remote Sens. Environ.*, vol. 61, no. 3, pp. 319–346, Sep. 1997.

[2] National Research Council; Board on Agriculture; Committee on Assessing Crop Yield, *Precision Agriculture in the 21st Century: Geospatial and Information Technologies in Crop Management*. Chicago, IL, USA: Footprint Books, 1998, p. 168.

[3] P. C. Robert, "Precision agriculture: A challenge for crop nutrition management," *Plant Soil*, vol. 247, no. 1, pp. 143–149, 2002.

[4] Z. Li, J. Wang, L. Bai, G. Jiang, S. Sun, P. Yang, and S. Wang, "Cotton yield estimation based on hyperspectral remote sensing in arid region of China," *Trans. Chin. Soc. Agricult. Eng.*, vol. 27, no. 6, pp. 176–181, 2011.

[5] N. H. Broge and J. V. Mortensen, "Deriving green crop area index and canopy chlorophyll density of winter wheat from spectral reflectance data," *Remote Sens. Environ.*, vol. 81, no. 1, pp. 45–57, Jul. 2002.

[6] P. M. Hansen and J. K. Schjoerring, "Reflectance measurement of canopy biomass and nitrogen status in wheat crops using normalized difference vegetation indices and partial least squares regression," *Remote Sens. Environ.*, vol. 86, no. 4, pp. 542–553, Aug. 2003.

[7] M. Shibuyama and T. Akiyama, "A spectroradiometer for field use. VII radiometric estimation of nitrogen levels in field rice canopies," *Jpn. J. Crop Sci.*, vol. 55, no. 4, pp. 439–445, 1986.

[8] L. Tarpley, K. R. Reddy, and G. F. Sassenrath-Cole, "Reflectance indices with precision and accuracy in predicting cotton leaf nitrogen concentration," *Crop Sci.*, vol. 40, no. 6, p. 1814, 2000.

[9] X. Yao, Y. Zhu, Y. Tian, W. Feng, and W. Cao, "Exploring hyperspectral bands and estimation indices for leaf nitrogen accumulation in wheat," *Int. J. Appl. Earth Observ. Geoinf.*, vol. 12, no. 2, pp. 0–100, 2009.

[10] Y. Ryu, D. D. Baldocchi, J. Verfaillie, S. Ma, M. Falk, I. Ruiz-Mercado, T. Hehn, and O. Sonnentag, "Testing the performance of a novel spectral reflectance sensor, built with light emitting diodes (LEDs), to monitor ecosystem metabolism, structure and function," *Agricult. Forest Meteorol.*, vol. 150, no. 12, pp. 1597–1606, Dec. 2010.

[11] O. M. B. Saeed, S. Sankaran, A. R. M. Shariff, H. Z. M. Shafri, R. Ehsani, M. S. Alfatni, and M. H. M. Hazir, "Classification of oil palm fresh fruit bunches based on their maturity using portable four-band sensor system," *Comput. Electron. Agricult.*, vol. 82, pp. 55–60, Mar. 2012.

[12] P. A. Larbi, R. Ehsani, M. Salyani, J. M. Maja, A. Mishra, and J. C. Neto, "Multispectral-based leaf detection system for spot sprayer application to control citrus psyllids," *Biosyst. Eng.*, vol. 116, no. 4, pp. 509–517, Dec. 2013.

[13] T. Fricke and M. Wachendorf, "Combining ultrasonic sward height and spectral signatures to assess the biomass of legume–grass swards," *Comput. Electron. Agricult.*, vol. 99, pp. 236–247, Nov. 2013.

[14] Y. Ryu, G. Lee, S. Jeon, Y. Song, and H. Kimm, "Monitoring multilayer canopy spring phenology of temperate deciduous and evergreen forests using low-cost spectral sensors," *Remote Sens. Environ.*, vol. 149, pp. 227–238, Jun. 2014.

[15] I. Moya, "A new instrument for passive remote sensing1. Measurements of sunlight-induced chlorophyll fluorescence," *Remote Sens. Environ.*, vol. 91, no. 2, pp. 186–197, May 2004.

[16] I. Moya, L. Camenen, G. Latouche, C. Mauxion, S. Evain, and Z. Cerovic, "An instrument for the measurement of sunlight excited plant fluorescence," in *Photosynthesis: Mechanisms and Effects*. Cham, Switzerland: Springer, 1998, pp. 4265–4270.

[17] Z. Zhong, M. Li, H. Sun, L. Wu, and Q. Wu, "Development and application of a smart apparatus for detecting crop nutrition," *Trans. Chin. Soc. Agricult. Machinery*, vol. 44, no. z2, pp. 215–219, 2013.

[18] J. Ni, X. Yao, Y. Tian, W. Cao, and Y. Zhu, "Design and experiments of portable apparatus for plant growth monitoring and diagnosis," *Trans. Chin. Soc. Agricult. Eng.*, vol. 29, no. 6, pp. 150–156, 2013.

[19] J. Ni, J. Dong, J. Zhang, F. Pang, W. Cao, and Y. Zhu, "The spectral calibration method for a crop nitrogen sensor," *Sensor Rev.*, vol. 36, no. 1, pp. 48–56, Jan. 2016.

[20] A. M. Ali, H. S. Thind, Varinderpal-Singh, and Bijay-Singh, "A framework for refining nitrogen management in dry direct-seeded rice using GreenSeeker optical sensor," *Comput. Electron. Agricult.*, vol. 110, pp. 114–120, Jan. 2015.

[21] J. Shen, Y. Miao, Q. Cao, H. Wang, W. Yu, S. Hu, H. Wu, J. Lu, X. Hu, W. Yang, and F. Liu, "Estimating rice nitrogen status using active canopy sensor crop circle 430 in northeast China," in *Proc. 3rd Int. Conf. Agro-Geoinformatics*, Aug. 2014, pp. 1–7.

[22] O. M. B. Saeed, S. Sankaran, A. R. M. Shariff, H. Z. M. Shafri, R. Ehsani, M. S. Alfatni, and M. H. M. Hazir, "Classification of oil palm fresh fruit bunches based on their maturity using portable four-band sensor system," *Comput. Electron. Agricult.*, vol. 82, pp. 55–60, Mar. 2012.

[23] O. S. Walsh, A. R. Klatt, J. B. Solie, C. B. Godsey, and W. R. Raun, "Use of soil moisture data for refined GreenSeeker sensor based nitrogen recommendations in winter wheat (triticum Aestivum L.)," *Precis. Agricult.*, vol. 14, no. 3, pp. 343–356, Jun. 2013.

[24] S. M. Samborski, D. Gozdowski, O. S. Walsh, D. W. Lamb, M. Stępień, E. S. Gacek, and T. Drzazga, "Winter wheat genotype effect on canopy reflectance: Implications for using NDVI for in-season nitrogen topdressing recommendations," *Agronomy J.*, vol. 107, no. 6, pp. 2097–2106, Nov. 2015.

[25] Q. Cao, Y. Miao, H. Wang, S. Huang, S. Cheng, R. Khosla, and R. Jiang, "Non-destructive estimation of rice plant nitrogen status with crop circle multispectral active canopy sensor," *Field Crops Res.*, vol. 154, pp. 133–144, Dec. 2013.

[26] J. Lu, Y. Miao, W. Shi, J. Li, and F. Yuan, "Evaluating different approaches to non-destructive nitrogen status diagnosis of rice using portable RapidSCAN active canopy sensor," *Sci. Rep.*, vol. 7, no. 1, p. 14073, Dec. 2017.

[27] Y. Zhu, Y. Li, W. Feng, Y. Tian, X. Yao, and W. Cao, "Monitoring leaf nitrogen in wheat using canopy reflectance spectra," *Can. J. Plant Sci.*, vol. 86, no. 4, pp. 1037–1046, Oct. 2006.

[28] F. Wei, Z. Yan, T. Yongchao, C. Weixing, Y. Xia, and L. Yingxue, "Monitoring leaf nitrogen accumulation in wheat with hyper-spectral remote sensing," *Acta Ecologica Sinica*, vol. 28, no. 1, pp. 23–32, Jan. 2008.

[29] Y. Zhu and W. Cao, "Quantitative relationship between leaf nitrogen accumulation and canopy reflectance spectra in wheat.," *J. Plant Ecol.*, vol. 30, no. 6, pp. 983–990, 2006.

[30] Z. Wu and X. Bao, "Monitoring leaf nitrogen accumulation with canopy spectral reflectance in rice," *Can. J. Plant Sci.*, vol. 32, no. 9, pp. 1316–1322, Jan. 2006.

[31] H. D. Hristov and J. M. Rodriguez, "Design equation for multidielectric fresnel zone plate lens," *IEEE Microw. Wireless Compon. Lett.*, vol. 22, no. 11, pp. 574–576, Nov. 2012.

[32] A. Petosa and A. Ittipiboon, "Design and performance of a perforated dielectric Fresnel lens," *IEE Proc.-Microw., Antennas Propag.*, vol. 150, no. 5, pp. 309–314, Oct. 2003.

[33] M. Kusko, A. Avram, and D. Apostol, "Design and fabrication of fresnel lenses," in *Proc. Int. Semiconductor Conf.*, 2008, pp. 445–448.

[34] G. Lemaire, M.-H. Jeuffroy, and F. Gastal, "Diagnosis tool for plant and crop N status in vegetative stage: Theory and practices for crop N management," *Eur. J. Agronomy*, vol. 28, no. 4, pp. 614–624, 2008.

[35] J. Jiang, C. Wang, Y. Wang, Q. Cao, Y. Tian, Y. Zhu, W. Cao, and X. Liu, "Using an active sensor to develop new critical nitrogen dilution curve for winter wheat," *Sensors*, vol. 20, no. 6, p. 1577, Mar. 2020.

[36] C.-W. Chang, D. A. Laird, M. J. Mausbach, and C. R. Hurburgh, "Near-infrared reflectance spectroscopy-principal components regression analyses of soil properties," *Soil Sci. Soc. Amer. J.*, vol. 65, no. 2, pp. 480–490, Mar. 2001.

[37] D. W. Lamb, M. G. Trotter, and D. A. Schneider, "Ultra low-level airborne (ULLA) sensing of crop canopy reflectance: A case study using a CropCircle sensor," *Comput. Electron. Agricult.*, vol. 69, no. 1, pp. 86–91, Nov. 2009.

[38] R. E. E. Jongschaap and R. Booij, "Spectral measurements at different spatial scales in potato: Relating leaf, plant and canopy nitrogen status," *Int. J. Appl. Earth Observ. Geoinf.*, vol. 5, no. 3, pp. 205–218, Sep. 2004.

[39] V. Sarlikioti, E. Meinen, and L. F. M. Marcelis, "Crop reflectance as a tool for the online monitoring of LAI and PAR interception in two different greenhouse crops," *Biosystems Eng.*, vol. 108, no. 2, pp. 114–120, Feb. 2011.

[40] K. Erdle, B. Mistele, and U. Schmidhalter, "Comparison of active and passive spectral sensors in discriminating biomass parameters and nitrogen status in wheat cultivars," *Field Crops Res.*, vol. 124, no. 1, pp. 74–84, Oct. 2011.

LILI YAO received the B.E. degree in electronic engineering from Anhui Polytechnic University, Wuhu, China, in 2015. He is currently pursuing the Ph.D. degree with the National Engineering and Technology Center for Information Agriculture, Nanjing Agricultural University. His research interests include crop field sensors, agricultural robotics, and agricultural automation.

RUSONG WU received the M.S. degree from Nanjing Agricultural University, Nanjing. His research interests include optical analysis and optical sensor design.

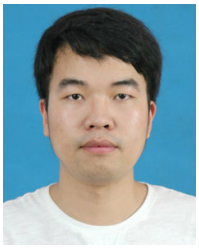

SHUN WU received the M.S. degree from Nanjing Agricultural University. His research interests include electronic information engineering and microcomputer embedded system.

XIAOPING JIANG received the Ph.D. degree from the Institute of Agricultural Engineering, Jiangsu University, Zhenjiang, China. He is currently a Researcher with the National Engineering and Technology Center for Information Agriculture. His current research interests include agricultural machinery and agricultural intelligent equipment.

YAN ZHU received the Ph.D. degree in agricultural informatics from Nanjing Agricultural University, in 2013. She is currently a Professor with the National Engineering and Technology Center for Information Agriculture, Nanjing Agricultural University. She is also the Dean of the Agricultural College, Nanjing Agricultural University, and the Director of the National Information Agricultural Engineering Technology Center. Her current research interests include crop modeling, agricultural informatics, crop cultivation, and farming technology.

WEIXING CAO received the Ph.D. degree in crop science from Oregon State University, in 1989. He is currently a Professor with Nanjing Agricultural University. He is also the Dean of the Intelligent Agricultural Research Institute, Nanjing Agricultural University, and the leader of the National Agricultural Professional Degree Collaboration Group in Agricultural Engineering and Information Technology, China. His current research interests include crop ecology, agricultural informatics, crop physiology, and crop cultivation.

JUN NI received the Ph.D. degree from the Institute of Agricultural Engineering, Jiangsu University, Zhenjiang, China. He is currently a Professor with the National Engineering and Technology Center for Information Agriculture, Engineering Research Center of Smart Agriculture, Ministry of Education, Key Laboratory for Crop System Analysis and Decision Making, Ministry of Agriculture and Rural Affairs, Jiangsu Key Laboratory for Information Agriculture, Jiangsu Collaborative Innovation Center for the Technology and Application of Internet of Things, Nanjing Agricultural University, China. His current research interests include crop information perception and processing, agricultural sensor, and intelligent equipment.